

# Effect of Selenium on Fluoride-Induced Changes in Synaptic Plasticity in Rat Hippocampus

Wei Qian · Keke Miao · Tao Li · Zigui Zhang

Received: 3 June 2013 / Accepted: 24 July 2013 / Published online: 21 August 2013  
© Springer Science+Business Media New York 2013

**Abstract** This study was conducted to further explore the effect of selenium on fluoride-induced changes in the synaptic plasticity in rat hippocampus. Animals were randomly divided into control group, F group (sodium fluoride: 50 mg/L), three Se groups (sodium selenite: 0.375, 0.75, and 1.5 mg/L), and three F+Se groups (sodium fluoride: 50 mg/L; sodium selenite: 0.375, 0.75, and 1.5 mg/L) and subjected to an exposure time of 6 months. The changes in synaptic plasticity in rat hippocampus were observed by electron microscopy. Compared with the fluoride group, the length of the synaptic active zone and the thickness of the postsynaptic density (PSD) increased significantly, whereas the width of the synaptic cleft decreased with high significance in the F+Se (0.75 mg/L) group. Moreover, the nitric oxide synthase activity and the nitric oxide content in the hippocampus decreased significantly in the F+Se (0.75 and 1.5 mg/L) groups. Furthermore, reverse transcriptase polymerase chain reaction and Western blot analyses showed that postsynaptic density-93 (PSD-93) expression in the hippocampus was increased significantly, whereas postsynaptic density-95 (PSD-95) expression decreased significantly in the fluoride group compared with the control group. The PSD-93 expression was inhibited in the three F+Se groups, whereas the opposite result was observed in PSD-95 expression. Based on the results, the optimal selenium dosage range that can antagonize the neurotoxicity of fluorosis is from 0.75 to 1.5 mg/L. The changes in PSD-93 expression may be the key factor to fluoride-induced central nervous toxicity and the effect of selenium intervention.

**Keywords** Fluoride · Selenium · Hippocampus · Brain damage · Antagonistic

W. Qian · K. Miao · T. Li · Z. Zhang (✉)  
College of Chemistry and Life Science, Zhejiang Normal University,  
Jinhua, Zhejiang 321004, People's Republic of China  
e-mail: zzg@zjnu.cn

## Introduction

Excessive fluoride ingestion over a prolonged period can have toxic effects on human and animal health. In addition to the well-known effects of fluorosis on the skeleton and teeth, the neurotoxicity of fluoride has also been confirmed. Chronic exposure to fluoride has been linked to learning disabilities and memory deficits [1]. Furthermore, studies show that fluoride has a specific effect on protein synthesis in the brain [2], which causes a decrease in the number of synapses, as well as significant changes in hippocampal morphology [3, 4]. Chronic exposure also alters the neurotransmitter and activities of some enzymes in the brain [5–7] and diminished the general cognitive capacities [8]. The hippocampus is the key region for learning and memory in the brain and the target tissue of fluoride neurotoxicity [9].

The synaptic potentiation and transmission were known to be dependent on nitric oxide (NO)-mediated signaling pathways [10]. NO contributes to many forms of learning-related synaptic plasticity including long-term potentiation and long-term depression in hippocampus [11]. NO is a catalyst synthesized by nitric oxide synthase (NOS), thus, the changes in NOS activity are related to the NO content. Postsynaptic density-93 (PSD-93) and postsynaptic density-95 (PSD-95) both are important representatives of the guanylate kinase protein family in hippocampus. PSD-95 is a synaptic scaffolding protein with multiple protein–protein interaction domains that is enriched in the postsynaptic density [12]. And PSD-93 belongs to the PSD-95 family proteins which shares similar domain structures in synapse [12].

In recent years, increased attention has been directed towards the protective effect of selenium against diseases of the nervous system. Selenium, a potent antioxidant, constitutes an essential component of glutathione peroxidase (GSH-Px) [13]. Selenium is both an essential and potentially toxic element for animals and humans; the protective mechanism of selenium might be related to its key roles in redox regulation

and antioxidant functions [14]. Selenium in appropriate concentrations has been found to alleviate fluorosis, promote the excretion of urinary fluoride, restrain lipid peroxidation, adjust the disorder of free radicals, and elevate GSH-Px activity [15].

The present study further explores the effects of selenium on fluoride-induced plasticity changes in the synapses in rat hippocampus based on our previous experiments, from which we concluded that 1.5 mg/L was the optimum concentration for selenium to antagonize chronic fluoride [15, 16]. The results of this study provide a theoretical basis for the use of selenium as an efficient, low-toxicity, anti-fluoride drug.

## Materials and Methods

### Experimental Animal Treatment

Eighty newly weaned male Sprague Dawley rats weighing 70 to 90 g each were procured from the Experimental Animal Center of Zhejiang Province in China. The rats were randomly divided into eight groups with 20 animals per group. The first group served as control and received tap water (fluoride concentration <0.2 mg/L and selenium concentration <1 µg/L). The fluoride-treated group was administered with aqueous sodium fluoride (NaF, 50 mg/L). In the three selenium only groups, selenium was used as sodium selenite with concentrations of 0.375, 0.75, and 1.5 mg/L mixed in drinking water, respectively. The remaining groups received NaF (50 mg/L)+Se (at concentrations of 0.375, 0.75, and 1.5 mg/L, respectively). Table 1 summarizes the experimental conditions. All the rats were fed with a standard pellet diet (contains 0.2 mg/kg fluorine and 0.1 mg/kg selenium) and given water ad libitum for 6 months.

### Chemicals and Reagents

NaF solid, sodium selenite solid, NO and NOS kits (Jiancheng, Naijing, China), rabbit polyclonal antibodies against PSD-93, PSD-95, and β-actin (Santa Cruz, CA, USA), horseradish peroxidase-conjugated goat anti-rabbit IgG (Boyun Biotech,

Shanghai, China), bicinchoninic acid (BCA) protein assay kit (Beyotime, Haimen, China), total RNA isolation kit (SBS Genetech, Beijing, China), reverse transcriptase polymerase chain reaction (RT-PCR) PrimeScript II first-strand cDNA synthesis kit, dNTP mixture and tag enzyme (TAKARA, Dalian, China), and PSD-93, PSD-95, and β-actin primers were synthesized at Sangon Biotech (Shanghai, China). All of the other chemicals used in this experiment were obtained from local commercial sources.

### Observation of Hippocampal Synaptic Ultrastructure

Two rats were randomly selected from each group, and the brains were extracted after decapitation with the use of anesthesia. The rat brains were initially fixed in 2.5 % glutaraldehyde solution until they became slightly harder. The CA3 region in the rat hippocampus was separated based on the brain stereotaxic coordinates. An ultrathin section was prepared, and ten photos of Gray I (excitation) synapses in the hippocampus CA3 region were taken for each rat using a transmission electron microscopy (JEOL JEM-2010). The number of synapses was calculated using the image analysis software, Image-Pro Plus 5.1. The width of the synaptic cleft, thickness of the postsynaptic density, length of the synaptic active zone, and curvature of the synaptic interface were measured using the double-blind method [17].

The synapse density ( $N_v$ ) was quantitatively analyzed using a tridimensional metrological method. A tissue in unit area was chosen as the reference system. The following formulas were used in the calculation [18]:  $N_v = 8EN_a/\pi^2$  (where  $N_a$  is the number of synapses in the unit area, and  $E$  is the average of the reciprocal of the postsynaptic density (PSD) length) and  $N_a = \sum N_x / \sum A_r$  (where  $N_x$  is the number of synapses in each photo, and  $A_r$  is the area of each photo).

### Determination of NO Content and NOS Activity

The rats were killed by decapitation with the use of anesthesia, and their hippocampuses were rapidly removed and weighed. A 10 % tissue homogenate with saline was produced and centrifuged at 1,000 rpm for 5 min. The supernatant was used in measuring the NO content in the hippocampus. The remaining homogenate was centrifuged at 3,500 rpm for 10 min, and the supernatant was used to measure the total NOS activity. The kits and experimental methods used were obtained from the Naijing Jiancheng Institute for Biomedical Research, China. The protein concentration in the tissue homogenate was measured using a BCA kit.

### Detection of PSD-93 and PSD-95 Protein Levels in Hippocampus by Western Blot Analysis

The hippocampus of the rat brain was dissected and stored at -70 °C until use. The tissue for membrane fraction was thawed

**Table 1** Experimental conditions for the different groups

Groups	Treatments
Con	Tap water (NaF<0.1 mg/L)
F	50 mg/L NaF
Se 0.375 (LSe)	0.375 mg/L Na <sub>2</sub> SeO <sub>3</sub>
Se 0.75 (MSe)	0.75 mg/L Na <sub>2</sub> SeO <sub>3</sub>
Se 1.5 (HSe)	1.5 mg/L Na <sub>2</sub> SeO <sub>3</sub>
F+low selenium (F+LSe)	50 mg/L NaF+0.375 mg/L Na <sub>2</sub> SeO <sub>3</sub>
F+moderate selenium(F+MSe)	50 mg/L NaF+0.75 mg/L Na <sub>2</sub> SeO <sub>3</sub>
F+high selenium (F+HSe)	50 mg/L NaF+1.5 mg/L Na <sub>2</sub> SeO <sub>3</sub>

and homogenized in ice-cold 0.32 M sucrose containing the protease inhibitor, phenylmethylsulfonyl fluoride (Beyotime, China), and centrifuged at  $800\times g$  for 10 min at 4 °C. The supernatant was collected in another centrifuge tube and then centrifuged at  $12,000\times g$  for 30 min at 4 °C to allow the sedimentation of crude membranes. The crude membrane pellet was suspended in 50 mM Tris-HCl to form a sample solution and then stored at -20 °C until processed for Western blot analysis. The protein concentration for each sample was estimated using a BCA protein assay kit. The protein sample solution was mixed with the buffer for sodium dodecyl sulfate (SDS)-polyacrylamide gel electrophoresis (PAGE) and denatured by boiling at 95 °C for 5 min in Laemmli sample buffer containing 5 %  $\beta$ -mercaptoethanol. Thirty micrograms of protein was run on 7.5 % SDS-PAGE gels and transferred to nitrocellulose membranes (Bio-Rad, Inc). After washing with a blocking solution (Tris-buffered saline with tween, TBST), the membranes were blocked for 2 h at room temperature with block solution (5 % milk in TBST). Subsequently, the blot was incubated with primary antibody (1:1,000 dilution of protein and 1:700 dilution of  $\beta$ -actin) at 4 °C overnight. The membranes were then washed and incubated with horseradish peroxidase-conjugated anti-rabbit IgG (1:7,000 of PSD-93 and 1:9,000 of  $\beta$ -actin, respectively) for 60 min. Finally, the membranes were incubated in electrochemiluminescence Plus reagent for 3 min. The signals were visualized by exposure to x-ray films. The images were inverted, and the Western blot intensity was determined using a computer image analysis system (Quantity One, Bio-Rad Laboratories).

#### Determination of PSD-93 and PSD-95 mRNA Levels by Reverse Transcriptase Polymerase Chain Reaction

For RT-PCR, total RNA was isolated from the hippocampus with Trizol according to the manufacturer's instructions. Total RNA (50  $\mu$ g) was subjected to reverse transcription using Random 6 mers under the following conditions: incubation at 30 °C for 10 min, 42 °C for 45 min, 95 °C for 5 min, and cooling on ice. Aliquots of cDNA were then amplified with each primer set for the PSD-93 genes (forward, 5'-GAAGTTACA CACGAAGAGGCTGT-3'; reverse, 5'-TCTCCACCCACAAT GTTGAA-3'), PSD-95 (forward, 5'-CATCTCCTTCATCCTT GCTG-3'; reverse, 5'-ATGTCATCGGTCTCACTGTC-3'), and GAPDH (forward, 5'-ATGGGAAGCTGGTCATCAAC-3'; reverse, 5'-GGATGCAGGGATGATGTTCT-3') in 20  $\mu$ L of reaction mixture containing 1  $\mu$ L dNTP mix (2.5 mM), 0.25  $\mu$ L Taq DNA polymerase (5 U/ $\mu$ L), 2  $\mu$ L 10 $\times$ buffer, 1  $\mu$ L MgCl<sub>2</sub> (25 mM), and a concentration of the 5'- and 3'-specific PCR primers. Reactions were performed for 35 cycles in a thermal cycler using melting, annealing, and extension cycling conditions at 94 °C for 30 s, 54 °C for 45 s, and 72 °C for 60 s. Amplified DNA fragments were subjected to electrophoresis on 1 % agarose gel and visualized by ethidium

bromide staining. The intensity of the bands was quantified with a densitometer. The intensities in each band resulting from PCR amplification were analyzed using image analysis software (Bio-Rad) to calculate the relative amounts of PSD-93 and PSD-95 vs. GAPDH cDNA.

#### Statistical Analysis

The data were represented as mean $\pm$ standard error ( $M\pm SE$ ). Mean values were determined using the homogeneity of variance test. If the variance passed the homogeneity test, the comparison of means was conducted using one-way analysis of variance, followed by the least significant difference post hoc test to compare the means of the different groups. All analyses were performed using SPSS 17.0 software.

## Results

### Measurements of Synaptic Density in Hippocampus

The synaptic density in the hippocampus was shown in Fig. 1, and the results of the measurements are shown in Table 2. Figure 1 showed the Gray I synapses in the control group observed by using electron microscope ( $\times 15000$ ). In Table 2, the synaptic density decreased significantly ( $P<0.05$ ) in the fluoride group compared with the control group. No statistically significant differences were found among the synaptic density of other groups ( $P>0.05$ ).

### Changes in the Synaptic Interface Submicrostructure Parameters in the Hippocampus

Different changes in the synaptic submicrostructure parameters were observed in each group. The photographs of the Gray I synapse in the hippocampus CA3 region in each group are shown in Fig. 2. Figure 2 panels a (control group) and c

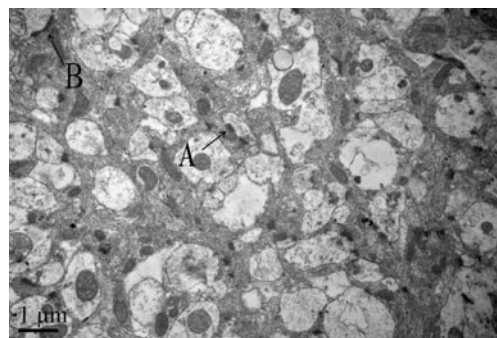


**Fig. 1** Synaptic structure under an electron microscope. **a** and **b** Gray I synapses. An ultrathin section was prepared, and photos of Gray I (excitation) synapses in the hippocampus CA3 region were taken using a transmission electron microscopy (JEOL JEM-2010). The synapse density was calculated using Image-Pro Plus 5.1

**Table 2** Synaptic density in the hippocampus in each group ( $M \pm SE$ )

Groups ( $n=50$ )	Density ( $N/\mu m^2$ )
Con	0.4878 $\pm$ 0.1810
F	0.3096 $\pm$ 0.2203*
LSe	0.3134 $\pm$ 0.1769
MSe	0.3324 $\pm$ 0.1264
HSe	0.4018 $\pm$ 0.1619
F+LSe	0.2948 $\pm$ 0.1234
F+MSe	0.3483 $\pm$ 0.2463
F+HSe	0.3478 $\pm$ 0.1285

Ten photos were taken from each rat and each group contained five rats. Data are presented as means $\pm$ SE. Mean values were determined using homogeneity test of variances and LSD test

\* $P < 0.05$ , compared with the control group

(LSe group) shows the existence of round vesicles in the presynaptic membrane of the rat hippocampus CA3 regions,

**Fig. 2** Electron microscopy images of the synaptic interface submicrostructure in the hippocampus CA3 region for each group ( $\times 100,000$ ). **a** Control group: synaptic structural integrity, vesicles clear and dense; **b** fluoride group: vesicles dispersed, structure blurred, width of synaptic cleft significantly widened, thickness of PSD thinned, and length of synaptic active zone shortened; **c** LSe group; **d** MSe group; **e** HSe group: length of synaptic active zone significantly shortened, organelles disordered, and curvature decreased; **f** F+LSe group; **g** F+MSe group: synaptic structural integrity, vesicles clear and dense; and **h** F+HSe group

significant thickening of the PSD material in the postsynaptic membrane, and a visible synaptic cleft. These characteristics coincided with the structural features of Gray I synapses (excitation synapses).

Figure 2b (fluoride group) shows the dispersed vesicles in the presynaptic membrane of the hippocampus, the blurred boundaries, shortened length of the synaptic active zone, significant widening of the width of the synaptic cleft, and the decrease in thickness of the PSD. The different selenium concentrations applied intervened with the fluoride-induced changes in the synaptic interface submicrostructure parameters in hippocampus at varying degrees.

The statistical data of the synaptic interface submicrostructure parameters in the hippocampus CA3 region are listed in Table 3. Compared with the control group, the length of the synaptic active zone and PSD thickness decreased highly significantly ( $P < 0.01$ ), and the width of the synaptic cleft increased highly significantly ( $P < 0.01$ ) in the fluoride group. However, the

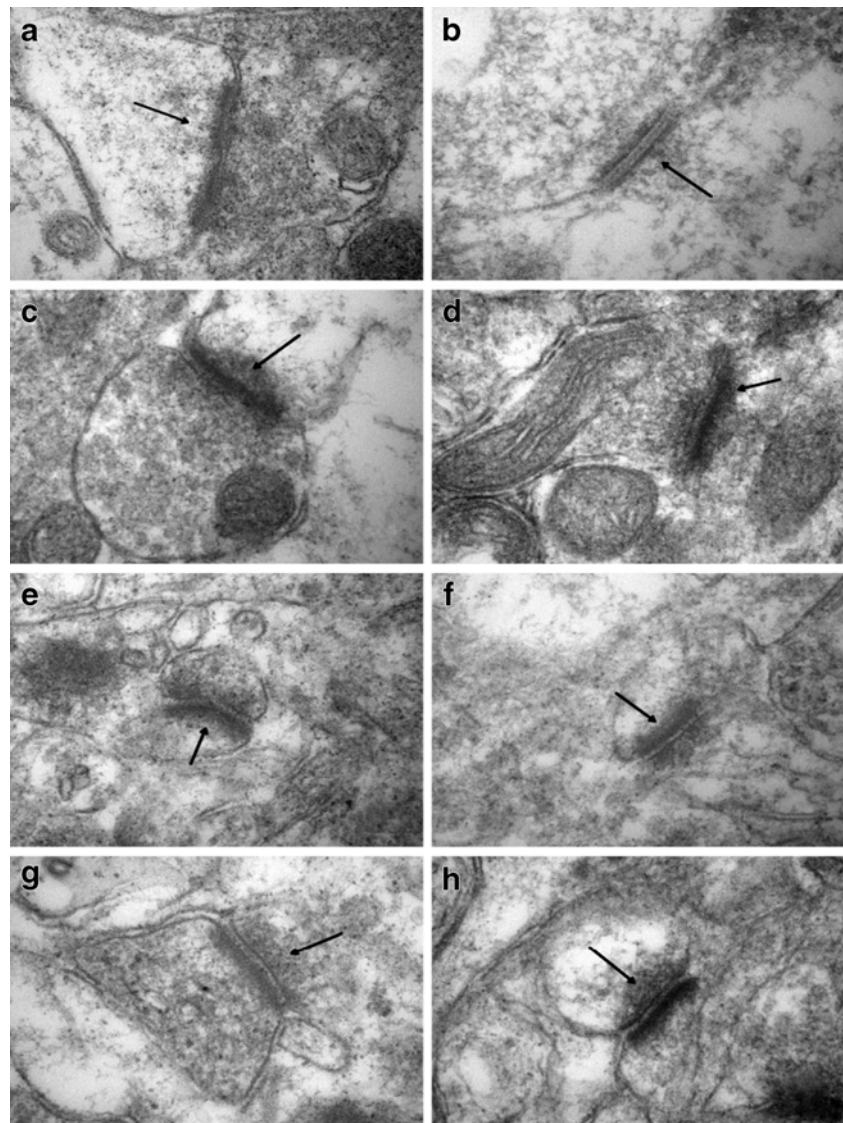


**Table 3** Synaptic interface submicrostructure parameters in the hippocampus CA3 region ( $M\pm SE$ )

Groups ( $n=50$ )	Length of synaptic active zone (nm)	Width of synaptic cleft (nm)	Thickness of PSD (nm)	Curvature of synaptic interface
Con	393.35 $\pm$ 138.48	16.12 $\pm$ 1.57	40.17 $\pm$ 8.35	0.93 $\pm$ 0.22
F	284.11 $\pm$ 68.68**	20.94 $\pm$ 6.36**	29.28 $\pm$ 4.57**	0.87 $\pm$ 0.08
LSe	316.16 $\pm$ 49.11	17.73 $\pm$ 3.24	34.70 $\pm$ 2.35	0.91 $\pm$ 0.13
MSe	307.61 $\pm$ 95.89	17.85 $\pm$ 5.20	34.81 $\pm$ 11.23	0.94 $\pm$ 0.11
HSe	302.67 $\pm$ 70.09*	18.22 $\pm$ 2.43	34.98 $\pm$ 6.32	0.93 $\pm$ 0.10
F+LSe	339.94 $\pm$ 52.60	19.27 $\pm$ 1.74	35.75 $\pm$ 8.53	0.91 $\pm$ 0.16
F+MSe	452.01 $\pm$ 107.13###	16.07 $\pm$ 2.23###	38.17 $\pm$ 3.00#	0.94 $\pm$ 0.04
F+HSe	320.66 $\pm$ 90.14	18.25 $\pm$ 4.02	36.96 $\pm$ 2.13#	0.89 $\pm$ 0.09

Ten synapses were calculated from each rat and each group contained five rats. Data are presented as means $\pm$ SE. Mean values were determined using homogeneity test of variances and LSD test

\* $P<0.05$ ; \*\* $P<0.01$ , compared with the control group

#  $P<0.05$ ; ###  $P<0.01$ , compared with the fluoride group

length of the synaptic active zone decreased significantly ( $P<0.05$ ) in the HSe group. Compared with the fluoride group, the length of the synaptic active zone increased highly significantly ( $P<0.01$ ), the width of the synaptic cleft decreased highly significantly ( $P<0.01$ ), and the thickness of PSD significantly increased ( $P<0.05$ ) in the F+MSe group. Similarly, the PSD thickness increased significantly ( $P<0.05$ ) in the F+HSe group.

#### Assay of NO Content and NOS Activity in the Hippocampus

The NO content and NOS activity in the hippocampus were evaluated. The statistical data are listed in Table 4. Compared with the control group, the NO content and NOS activity in the rat hippocampus increased highly significantly ( $P<0.01$ ) in the fluoride group, and the NOS activity significantly increased ( $P<0.05$ ) in the Se (Se 0.75 and 1.5 mg/L) and F+LSe groups.

**Table 4** NO content and NOS activity in hippocampus ( $M\pm SE$ )

Groups ( $n=10$ )	NO ( $\mu\text{mol/g prot}$ )	NOS ( $\text{u/mg prot}$ )
Con	0.34 $\pm$ 0.048	0.09 $\pm$ 0.003
F	0.72 $\pm$ 0.092**	0.44 $\pm$ 0.064**
LSe	0.53 $\pm$ 0.100	0.33 $\pm$ 0.078*
MSe	0.56 $\pm$ 0.120	0.32 $\pm$ 0.064*
HSe	0.55 $\pm$ 0.112	0.27 $\pm$ 0.106
F+LSe	0.52 $\pm$ 0.118	0.30 $\pm$ 0.101*
F+MSe	0.49 $\pm$ 0.068	0.10 $\pm$ 0.005###
F+HSe	0.42 $\pm$ 0.061#	0.11 $\pm$ 0.011###

Data are presented as means $\pm$ SE. Mean values were determined using homogeneity test of variances and LSD test

\* $P<0.05$ ; \*\* $P<0.01$ , compared with the control group

#  $P<0.05$ ; ###  $P<0.01$ , compared with the fluoride group

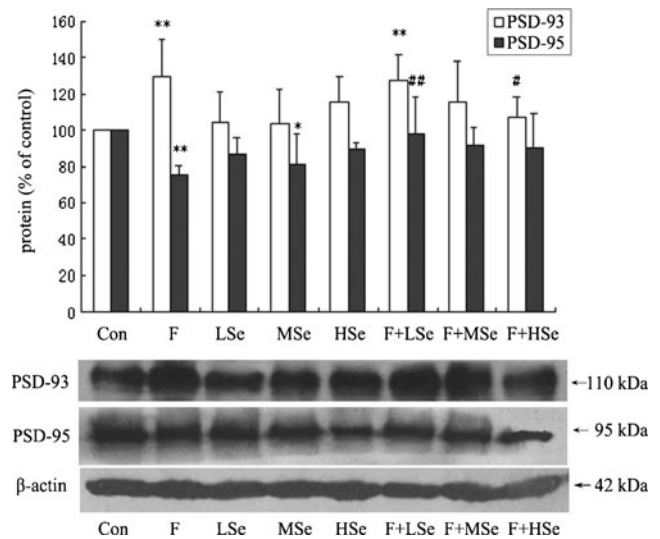


**Fig. 3** Changes in the protein levels of PSD-93 and PSD-95 in the hippocampus ( $M\pm SE$ ,  $n=3$ ). A Western blot analysis data and the quantification of band intensity are shown. The data are expressed as the ratio of the band intensity value to the corresponding  $\beta$ -actin optical density (OD). \* $P<0.05$ , \*\* $P<0.01$ , compared with the control group; # $P<0.05$ , ### $P<0.01$ , compared with the fluoride group

Compared with the fluoride group, NOS activity decreased highly significantly ( $P<0.01$ ) in the F+Se (Se 0.75 and 1.5 mg/L) groups. Moreover, NO content decreased significantly ( $P<0.05$ ) in the F+HSe group.

#### Western Blot Analysis of PSD-93 and PSD-95

The changes in the protein expressions of PSD-93 and PSD-95 in the hippocampus were detected using Western blot analysis, and the results are presented in Fig. 3. Compared with the control group, the protein expression of PSD-93 in rat hippocampus was highly significant ( $P<0.01$ ), which increased by 30 and 28 % in the fluoride and F+LSe groups, respectively. Compared with the fluoride group, the protein expression of PSD-93 significantly decreased ( $P<0.05$ ) by 18 % in the F+HSe group. The protein expression of PSD-95 decreased highly significantly ( $P<0.01$ ) by 25 % in the fluoride group, and significantly decreased ( $P<0.05$ ) by 19 % in the MSe group when compared with control group. Furthermore, the protein expression of PSD-95 increased highly significantly ( $P<0.01$ ) by 23 % in the F+LSe group when compared with the fluoride group.

#### RT-PCR Analysis of PSD-93 and PSD-95

The mRNA expression was detected by RT-PCR to examine the changes in the mRNA expression of PSD-93 and PSD-95 in the hippocampus. The results are shown in Fig. 4. Compared with the control group, the mRNA expression of PSD-93 in the rat hippocampus increased highly significantly ( $P<0.01$ ) by 34 % in the fluoride group. Compared with the

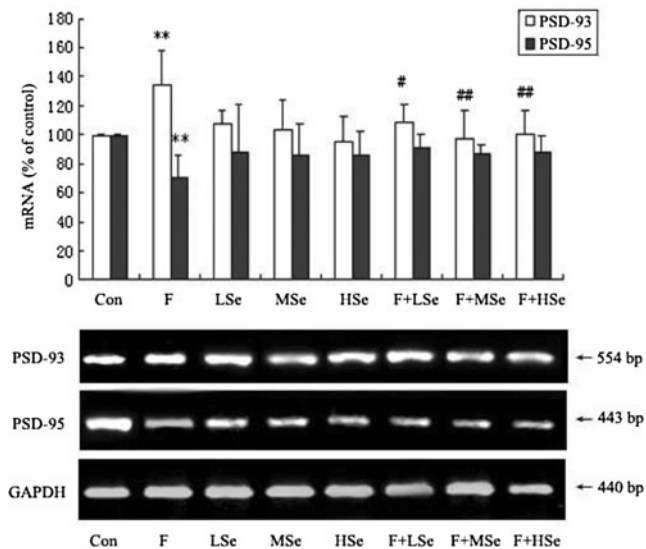


**Fig. 4** Changes in the mRNA expression levels of PSD-93 and PSD-95 in the hippocampus ( $M \pm SE$ ,  $n=3$ ). A semi-quantitative PCR analysis data and the quantification of band intensity are shown. The data are expressed as the ratio of the band intensity value to the corresponding  $\beta$ -actin optical density (OD). \* $P < 0.05$ , \*\* $P < 0.01$ , compared with the control group; # $P < 0.05$ , ## $P < 0.01$ , compared with the fluoride group

fluoride group, the mRNA expression of PSD-93 significantly decreased ( $P < 0.05$ ) by 19 % in the F+LSe group, and decreased highly significantly ( $P < 0.01$ ) by 27 and 25 % in the two F+Se groups (Se 0.75 and 1.5 mg/L, respectively).

Compared with the control group, the mRNA expression of PSD-95 decreased highly significantly ( $P < 0.01$ ) by 29 % in the fluoride group. However, compared with the fluoride group, the mRNA expression of PSD-95 tended to rise in all three F+Se groups, but no significant differences were observed ( $P > 0.05$ ).

## Discussion

Endemic fluorosis is a typical geochemical disease. Past studies on fluorosis focused on the damage to phrenological organs. Recent studies have found that chronic fluorosis induces injury in non-phrenological organs, especially to the central nervous system [19–21]. Selenium is an indispensable component of glutathione peroxidase and some antioxidant proteins. It can inhibit free radicals, enhance antioxidant capacities, maintain biofilm stability, and perform other important physiological functions [22, 23]. Selenium has both nutritional and poisonous properties—its biological effects depend largely on the administered dose [24]. The range between nutritional and toxic doses of selenium is narrow. When using selenium as a nutritional supplement, its safety limits and potential toxic effects are first considered [25]. Researchers have shown that selenium attenuates high concentrations of

fluoride of rats, promotes urinary fluoride excretions [26, 27], and alleviates symptoms of fluorosis. Studies have also shown that selenium in appropriate concentrations alleviates fluoride-induced injury to the central nervous system [28]. The current experiment is based on an effective selenium dose of 1.5 mg/L based on our previous studies of selenium against chronic fluorosis in adult fluorosis rats [15, 28]. However, the specific molecular mechanism remains unknown.

The hippocampus is closely related to learning, memory, and emotional behavior. The transmission of nerve signals and plasticity changes in synapses are easily affected by age [29], drugs [30], and environmental factors [4]. The morphological studies on nerve cells have shown that fluorosis can induce synaptic plasticity changes in the hippocampus, including the curvature of synaptic interface, width of synaptic cleft, PSD thickness, and length of the synaptic active zone [31]. These parameters are important factors affecting synaptic transmission efficiency [32, 33]. The results in this study indicated that a high fluoride level can induce pathological changes in the synaptic ultrastructure of the hippocampus, and intake of selenium alone may also induce damage to the central nervous system. These findings suggest that the accumulation of selenium due to excessive selenium supplementation may cause selenium poisoning. However, the results on the appropriate concentration of selenium intervening with fluoride-induced synaptic plasticity changes in the hippocampus are consistent with those of previous studies [28].

Epidemiological studies indicated that the cognitive deficits in fluorosis patients may be related to the fluoride-induced cellular signal transduction factor. As an endogenous free radical, NO generates strong oxidant peroxynitrite, induces lipid peroxidation, and damages the protein structure via the nitric oxide of amino acids. The NO content and metabolic regulation enzyme for NOS activity increased significantly, which generated subsequent neurotoxicity [34]. Furthermore, studies have demonstrated the location of NOS in brain neurons which suggests that NOS may be implicated in synaptic plasticity [35]. The increase of the NOS activity in fluoride and three selenium groups suggest that intake of selenium alone may have toxic effects on hippocampus. While the decrease of NOS activity in the F+Se (0.75 and 1.5 mg/L) group indicates that appropriate selenium concentrations can antagonize these changes. These results provide further evidence for the theory on fluoride-induced oxidative stress and nitrous acid damage [36, 37].

The PSD is the part of the cytoskeletal structure that organizes and mediates the signaling pathway of excitatory synaptic transmission. Its protein composition and changes are closely related to the postsynaptic effect [34, 38]. The complexes that form the series of proteins, including PSD-93 and PSD-95, mainly exist in the postsynaptic membrane of excited asymmetric type II synapses. PSD-93 and PSD-95 appear to have distinct roles in synaptic plasticity, perhaps through differential recruitment of signaling molecules to the *N*-methyl-*D*-aspartate

receptor (NMDAR) [39]. The destruction of PSD-93 weakened the NMDAR aggregation in the cell membrane, reduced neuronal nitric oxide synthase (nNOS) activity, and mediated the neurotoxicity by NMDAR–nNOS. Studies have indicated that excessive fluoride directly induces changes in the protein structure and activity, hinders the beginning of peptide chain synthesis, and significantly reduces the mRNA content and the rate of protein synthesis [34]. The increase of the protein and mRNA levels of PSD-93 in the hippocampus by fluorosis and the antagonism of fluoride-induced expression changes of PSD-93 under appropriate concentrations of selenium prompted the PSD-93 which may be key links to the fluoride-induced toxicity in the central nervous system and the intervention of selenium. PSD-95 spreads over the neuronal cell bodies and is closely related to physiological processes such as learning, memory, synaptic plasticity, and pathological damage due to ischemia and hypoxia [40, 41]. Although selenium mitigates the changes in PSD-95 expression with fluorosis, the effects are not significant.

Compared with the fluorosis-induced effects on the protein and gene expression levels of PSD-93 and PSD-95 in the rat hippocampus, the opposite trend in the expression levels was found, thus verifying that the outcome on synaptic plasticity by regulating either PSD-95 or PSD-93 levels is dramatically different [42]. The different protein expressions of PSD-93 between the control and the F+LSe group is likely because low selenium concentrations cannot attenuate the toxicity of fluoride. The appropriate selenium concentrations intervene in fluoride-induced changes in the protein and mRNA expression levels of PSD-93 and PSD-95 in the hippocampus. While the protein and gene expression levels of PSD-93 showed no significant differences among the three selenium groups, which suggested that selenium alone had different biological effects than those of combined selenium and fluoride.

In summary, chronic fluorosis caused injury to synaptic plasticity in rat hippocampus. The NO content, NOS activity, and changes in the gene and protein expression levels of PSD-93 and PSD-95 may provide the molecular basis for fluoride-induced changes in the synaptic plasticity in the hippocampus. The appropriate selenium concentration exhibited evident effects on the changes of the synaptic plasticity in the hippocampus induced by chronic fluorosis. The mechanism might be related to the reversal of fluoride-induced molecular changes in the synapses in the hippocampus under the experimental conditions. In our studies, the selenium concentration from 0.75 to 1.5 mg/L was the optimal dosage range for antagonizing the neurotoxicity of fluorosis in adult rats. But it needs further study, since higher concentration may also have prevention effect. The changes in the protein and gene expression levels of PSD-93 might be the key link to fluoride-induced central nervous toxicity and the intervention of selenium.

**Acknowledgments** This research was supported by the National Natural Science Foundation of China (no. 81273015).

**Conflict of Interest** None.

## References

- Sharma JD, Sohu D, Jain P (2009) Prevalence of neurological manifestation in a human population exposed to fluoride in drinking water. *Fluoride* 42(2):127–132
- Shivarajashankara YM, Shivashankara AR, Bhat PG et al (2002) Brain lipid peroxidation and antioxidant systems of young rats in chronic fluoride intoxication. *Fluoride* 35(3):197–203
- Shashi A (2003) Histopathological investigation of fluoride induced neurotoxicity in rabbits. *Fluoride* 36(2):95–105
- Bhatnagar M, Rao P, Sushma J et al (2002) Neurotoxicity of fluoride: neurodegeneration in hippocampus of female mice. *Indian J Exp Biol* 40(5):546–554
- Bhatnagar M, Rao P, Saxena A et al (2006) Biochemical changes in brain and other tissues of young adult female mice from fluoride in their drinking water. *Fluoride* 39(4):280–284
- Wu CX, Gu XL, Ge YM et al (2006) Effects of high fluoride and arsenic on brain biochemical indexes and learning-memory in rats. *Fluoride* 39(4):274–279
- Chirumari K, Reddy PK (2007) Dose-dependent effects of fluoride on neurochemical milieu in the hippocampus and neocortex of rat brain. *Fluoride* 40(2):101–110
- Xiang Q, Liang Y, Chen L et al (2003) Effect of fluoride in drinking water on children's intelligence. *Fluoride* 36(2):84–94
- Lu Y, Sun ZR, Wu LN et al (2000) Effect of high-fluoride water on intelligence in children. *Fluoride* 33(2):74–78
- Sho K, Masahiko S, Nozomu M (2012) Protein oxidation inhibits NO-mediated signaling pathway for synaptic plasticity. *Neurobiol Aging* 33(3):535–545
- Hawkins RD (2008) Transsynaptic signaling by NO during learning-related synaptic plasticity. *Learn Mem Compr Ref* 4:793–802
- Kihoon H, Eunjoon K (2008) Synaptic adhesion molecules and PSD-95. *Prog Neurobiol* 84:263–283
- Samah SO, Zeynab KE (2012) Protective effect of vitamin E and selenium combination on deltamethrin-induced reproductive toxicity in male rats. *Exp Toxicol Pathol* 64(7–8):813–819
- Lewin MH, Arthur JR, Riemersma RA et al (2002) Selenium supplementation acting through the induction of thioredoxin reductase and glutathione peroxidase protects the human endothelial cell line EAhy926 from damage by lipid hydroperoxides. *Biochim Biophys Acta* 1593(1):85–92
- Feng P, Wei JR, Zhang ZG (2011) Intervention of selenium on chronic fluorosis-induced injury of blood antioxidant capacity in rats. *Biol Trace Elem Res* 144(1–3):1024–1031
- Feng P, Wei JR, Zhang ZG (2012) Influence of selenium and fluoride on blood antioxidant capacity of rats. *Exp Toxicol Pathol* 64(6):565–568
- Essatara MB, Morley JE, Levine AS et al (1984) The role of the endogenous opiates in zinc deficiency anorexia. *Physiol Behav* 32(3):475–478
- Chen YC, Han TZ, Shen JX et al (1999) A quantitative study on the synaptic ultrastructural alterations in visual cortex in the maintenance of Itp. *Acta Physiol Sin* 51(1):73–79
- Kobayashi CA, Leite AL, Silva TL et al (2009) Proteomic analysis of kidney in rats chronically exposed to fluoride. *Chem-Biol Inter* 180(2):305–311
- Xiong XZ, Liu JL, He WH et al (2007) Dose-effect relationship between drinking water fluoride levels and damage to liver and kidney functions in children. *Environ Res* 103(1):112–116
- Zhu WJ, Zhang J, Zhang ZG (2011) Effects of fluoride on synaptic membrane fluidity and PSD-95 expression level in rat hippocampus. *Biol Tr Elem Res* 139(2):197–203

22. Luo HJ, Ji YH (2000) Biological role and significance of selenium. *Stud Trace Elem Health* 17(2):70–72
23. Han B, Yoon SS, Wu PF et al (2006) Role of selenium in alteration of erythrocyte parameters in bovine fluorosis. *Asian Australas J Anim Sci* 19(6):865–872
24. Abdella A, Gan L, Liu Q et al (2003) The antioxidation of breviscapine and its antagonist of selenium on liver toxicity in rat. *Chin Pharmacol Bull* 19(1):113–115
25. Wang GZ, Niu ZX (2011) The progress study of toxicity of selenium. *Northwest Pharm J* 25(3):237–238
26. Zhu WJ, Zhang ZG, Shen XY (2009) Pathogenesis of fluorosis and the role of selenium against fluoride. *Chin J Endemiol* 28(6):704–706
27. Holger S, Lirija A, Esra B et al (2006) Involvement of selenoprotein P in protection of human astrocytes from oxidative damage. *Free Radic Biol Med* 40(9):1513
28. Zhang ZG, Shen XY, Xu XL (2001) Effects of selenium on the damage of learning-memory ability of mice induced by fluoride. *J Hyg Res* 30(3):144–146
29. Frick KM, Fernandez SM (2003) Enrichment enhances spatial memory and increases synaptophysin levels in aged female mice. *Neurobiol Aging* 24(4):615–626
30. Xu XH (2003) Investigation on effects of puerarin against memory impairment in mice induced by chronic alcoholism. *Chin J Pharm* 38(1):31–34
31. Zhang ZG, Xu XL, Shen XY et al (1999) Effect of fluoride exposure on synaptic structure of brain areas related to learning–memory in mice. *J Hyg Res* 28(4):210–212
32. Wyneken U, Smalla KH, Marengo JJ et al (2001) Kainate-induced seizures alter protein composition and N-methyl-D-aspartic acid receptor function of rat forebrain postsynaptic densities. *Neuroscience* 102(1):65–74
33. Myried N, Zhang WN, Joram F et al (2007) Differential expression of PSD proteins in age-related spatial learning impairments. *Neurobiol Aging* 28(1):143–155
34. Shashi A, Singh JP, Thapar SP (1994) Effect of long-term administration of fluoride on levels of protein, free amino acids, and RNA in rabbit brain. *Fluoride* 27(3):155–159
35. Çiğdem GS, Serdar K, Orhan A et al (2012) Correlation between hippocampal levels of neural, epithelial, and inducible NOS and spatial learning skills in rats. *Behav Brain Res* 235(2):326–333
36. Hassan HA, Yousef MI (2009) Mitigating effects of antioxidant properties of black berry juice on sodium fluoride induced hepatotoxicity and oxidative stress in rats. *Food Chem Toxicol* 47(9):2332–2337
37. Mittal M, Flora SJ (2006) Effects of individual and combined exposure to sodium arsenite and sodium fluoride on tissue oxidative stress, arsenic, and fluoride levels in male mice. *Chem Biol Interact* 162(2):128–139
38. Boeckers TM (2006) The postsynaptic density. *Cell Tissu Res* 326(2):409–422
39. Holly JC, Ann EF, Seth GN et al (2008) Opposing effects of PSD-93 and PSD-95 on long-term potentiation and spike timing-dependent plasticity. *J Physiol* 586(24):5885–5900
40. Lin CS, Tao PL, Jong YJ et al (2009) Prenatal morphine alters the synaptic complex of postsynaptic density 95 with N-methyl-aspartate receptor subunit in hippocampal CA1 subregion of rat offspring leading to long-term cognitive deficits. *Neuroscience* 158(4):1326–1337
41. Du CP, Gao J, Tai JM et al (2009) Increased tyrosine phosphorylation of PSD-95 by Src family kinases after brain ischemia. *J Biochem* 417(1):277–285
42. Xu WF (2011) PSD-95-like membrane associated guanylate kinases (PSDMAGUKs) and synaptic plasticity. *Curr Opin Neurobiol* 21(2):306–312